Highly efficient tabletop x-ray laser at $\lambda = 41.8$ nm in Pd-like xenon pumped by optical-field ionization in a cluster jet

E. P. Ivanova
Institute of Spectroscopy, Russian Academy of Sciences, 142190 Troitsk, Moscow Region, Russian Federation
(Received 26 April 2011; published 19 October 2011)

The atomic-kinetic calculations of gain at 41.8 nm in Pd-like xenon are performed. The interpretation of known experiments has proved that x-ray laser in Pd-like xenon is feasible in the extremely wide range of atomic densities: $10^{17} \leqslant [Xe^{8+}] \leqslant 3 \times 10^{19}$ cm^{-3}. This result is due to the large cross sections (and rates) of level excitations in Pd-like xenon by electron impact. We propose a highly efficient tabletop x-ray laser pumped by optical-field ionization in a xenon cluster jet. The efficiency of ~0.5% is possible with a pump laser pulse energy of $\geqslant$0.001 J and an intensity of $\sim 10^{16}$ W/cm^2.

DOI: 10.1103/PhysRevA.84.043829 PACS number(s): 42.55.Vc, 52.38.Ph

I. INTRODUCTION

A new class of electron-excited x-ray lasers was proposed by Burnett and Corkum [1] in which an intense circularly polarized femtosecond laser pulse is used to tunnel ionize a gaseous target producing plasmas with hot electrons necessary to collisionally pump the x-ray lasers (XRL). The simulation of three XRL schemes in noble-gas targets was performed in Ref. [2]. These systems were longitudinally and differentially pumped along cells by circularly polarized femtosecond laser pulses focused to an intensity of 10^{16}–10^{17} W/cm^2. The simulation predicted high gains in all three systems: $2p^53p\ ^1S_0$–$2p^53s\ ^1P_1$ in Ne-like Ar (Ar $^{8+}$) at $\lambda = 46.9$ nm; $3d^94d\ ^1S_0$–$3d^94p\ ^1P_1$ in Ni-like krypton (Kr^{8+}) at $\lambda = 32.8$ nm and $4d^95d\ ^1S_0$–$4d^95p\ ^1P_1$ in Pd-like xenon (Xe^{8+}) at $\lambda = 41.8$ nm. Since the past two decades there has been much interest in developing optical-field ionization (OFI) XRL. The principal objectives are to reduce the size and to increase repetition rates, as well as to achieve a large yield of extreme ultraviolet radiation.

The first electron collisionally pumped OFI XRL was reported in Ref. [3], where a 10 Hz, 70 mJ circularly polarized laser pulse with a 40-fs-long time duration was longitudinally focused in a cell containing xenon gas at a pressure ranging from 5 to 12 torr. It was not possible to directly measure the focused spot size in which the plasma was likely to affect laser beam propagation. However, from the observed ion stages, the peak intensity was deduced to be higher than 3×10^{16} W/cm^2 over a length $L \sim 7.4$ mm. The gain region was estimated in Ref. [3] between 50 and 100 μm. The saturation at $L \sim 7.4$ mm was not obtained; the numerical data for the yield into the line at 41.8 nm were not measured. The gain-length product was estimated in Ref. [3] as $gL \approx 11$.

The first saturated over L OFI XRL at 41.8 nm in Xe^{8+} was demonstrated in Ref. [4] by focusing a 330 mJ, 10 Hz, 35 fs, circularly polarized laser pulse into a gas cell filled with 15 torr of xenon. The pulse was focused with an $f = 1000$ mm normal incidence spherical mirror, resulting in a nearly Airy distribution in the focal plane, with a central spot 40 μm in diameter that includes 40% of the total energy. The resulting average pulse intensity was up to $I_{pump} \sim 3 \times 10^{17}$ W/cm^2. The contrast ratio was measured to be $>10^6$. About 5×10^9 photons per pulse (N_{out}^{ph})have been produced and a $gL \approx 15$ has been inferred to demonstrate an amplification saturated over $L \approx 5$ mm.

The XRL pumped by OFI in a cluster jet was demonstrated in Ref. [5]. A 10 TW, 55 fs, 810 nm, 10 Hz Ti:sapphire laser system was used in Ref. [5]. A concave mirror of 1 m focal length was used for pump pulse focusing. The focal spot size of the pump pulse was 25 μm in full width at half maximum with 85% energy enclosed in a Gaussian profile. The peak intensity reached 7×10^{17} W/cm^2 for a pump energy of 350 mJ. There were two different nozzles used for cluster jet formation. One was a conical nozzle with a 6 mm outlet diameter, a 1.2 mm throat diameter, and a 5.4° opening angle, producing a jet profile. The average cluster size was estimated to be 15–50 nm for a backing pressure of 0.7–4 MPa. The corresponding average atom density was measured to be 1.1×10^{17} to 6.9×10^{17} cm^{-3}. The second was a slit nozzle with an outlet of 5×0.5 mm dimensions. The jet profile had a flattop region 3.5 mm in length and a sharp boundary. The average atom density was measured to be 1.1×10^{17} to 3.3×10^{19} cm^{-3} for a backing pressure of 0.013–4 MPa (0.13–40 atm). Two ways of pumping were investigated for both types of nozzle, i.e., with and without prepulse. The striking result was that strong lasing was observed in an experiment with a slit nozzle without prepulse for plasma density ranging by more than two orders of magnitude. A special Rayleigh scattering study proved that nanoplasma in a cluster was formed under the influence of the pedestal of the femtosecond pulse. The pedestal length was estimated to be 1.5–3 ns. The early initiation of the nanoplasma expansion for the slit nozzle was believed to result from different cluster sizes in comparison with the conical nozzle. The maximal energy of the 41.8 nm lasing line reached 95 nJ ($N_{out}^{ph} = 2 \times 10^{10}$ photons/pulse) at average atom density 7.5×10^{17} cm^{-3}, i.e., the N_{out}^{ph} was larger than in the experiment [4] by a factor of 4.

In all three experiments, the lasing output was sensitive to pump pulse polarization, and the best results were achieved using circular polarization. In all experiments, the ionization-induced refraction resulted in defocusing of the pump pulse, as well as in the radial nonuniformity of the plasma column. Experimental demonstrations of high gains [3–5] require a detailed theoretical interpretation to simulate the conditions for the highly efficient XRL.

In this study, we perform atomic-kinetic calculations of gain [$g(t)$] on the transition $4d^95d\ ^1S_0$–$4d^95p\ ^1P_1$ at $\lambda = 41.8$ nm in

the Pd-like xenon. We simulate lasing in plasma to reproduce the experimental dependence on plasma length (comparison with [3–5]), as well as the dependence on xenon density (comparison with [5]) by adjusting the plasma parameters. We explain the cause of the anomalously wide range of the electron (ion) density for the XRL.

The interpretations of the XRL pumped by OFI of gaseous xenon targets are necessary to test our model. The interpretation of the XRL pumped by OFI in a cluster jet along with an analysis of the way to obtain the maximum possible yield is aimed to justify the principles of highly efficient tabletop XRL at 41.8 nm. The idea is based on obtaining optimal electron density, temperature, and plasma geometry with a properly chosen cluster size. Additionally, it is important to optimize the parameters of the pumping laser pulse: the duration and intensities of the pedestal, as well as the intensity of the main femtosecond (or picosecond) pulse.

II. THEORETICAL MODEL

There are at least two reasons why the femtosecond pulse-driven XRL is a favorable approach to test theory: (i) the plasma density and length are known and (ii) the ionization balance is almost 90% of Xe^{8+} if I_{pump}, E_{pump}, and the driving pulse pedestal are chosen correctly. Moreover, simplification is due to the fact that an active medium is formed almost instantaneously after the pump pulse action [2,3].

The laser transition at $\lambda = 41.81$ nm is shown in Fig. 1. The atomic-kinetic calculations are performed assuming plasma homogeneity; in this case, the following five parameters are sufficient for the gain calculation: electron and ionic densities n_e and n_i, temperatures T_e and T_i, and the plasma filament diameter d. To calculate the gain g at the line center we will use the known expression (see, e.g., [6])

$$g = A_{ul}\lambda^2[N_{\text{up}} - (g_u/g_l)N_{\text{low}}]/8\pi\,\Delta\nu_0, \qquad (1)$$

where A_{ul} is the probability of the radiative transition between the upper (u) and lower (l) levels, λ is the transition wavelength, $N_{\text{up}} = n_i P_{\text{up}}$ and $N_{\text{low}} = n_i P_{\text{low}}$ are the concentrations of ions in the upper and lower active states, respectively, P_{up} and P_{low} are the upper- and lower-level populations, respectively, and g_{up} and g_{low} are the statistical weights of the upper and lower levels, respectively. The transition line profile is determined by the convolution of the Doppler and natural profiles. The latter

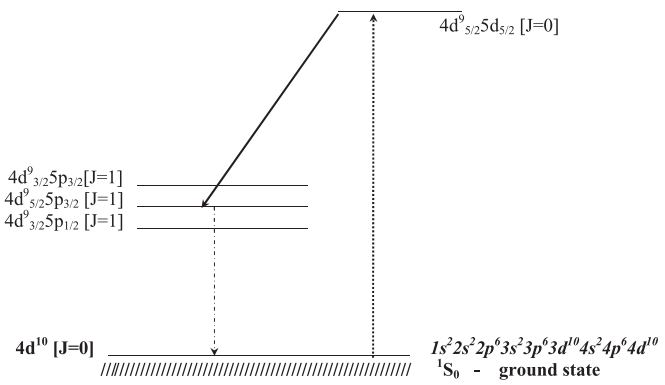

FIG. 1. Laser transition at 41.81 nm in Pd-like xenon (Xe^{8+}).

is due to the radiation transitions and collisional processes, which relate each level to all other levels of Xe^{8+} and to the ion in the adjacent ionization stage. $\Delta\nu_0$ is the linewidth at the center (Voigt profile); it is determined by the simplified method proposed in Ref. [6]. The assumption on energy distributions of electrons is given in Table I.

Level populations for Xe^{8+} and $g(t)$ are determined by solving the kinetic equations for level populations. We assume that plasma parameters remain constant during a relatively short (5–10 ps) XRL pulse. Our approach to solve the atomic-kinetic problem can be found in recent papers [7,8] (and references therein). All atomic data are calculated by the relativistic perturbation theory with model potential of zero approximation (RPTMP). In Table I, the transition probabilities, calculated by RPTMP, are compared to the corresponding data, calculated in Ref. [2]. The probabilities of radiative transitions from an upper to a lower active level and from a low active level to the ground level are in agreement within 20–30 %. The rates of electron-induced transitions and linewidths are in satisfactory agreement, except for the rate of collisional excitation of the lower and upper active levels $4d^9 5p\ ^1P_1$ and $4d^9 5d\ ^1S_0$ from the ground level. The theoretical value of $g \sim 107$ in Ref. [2] is approximately an order of magnitude higher than the experimentally determined value of g. We conclude that the large disagreement of the theoretical [2] and experimental [3] values of gain is caused by too large rates of electron-induced transitions from the ground level in Ref. [2]. Note that too simplified calculations of the gain can lead to large errors.

III. INTERPRETATION OF THE X-RAY LASERS IN Xe^{8+} PUMPED BY OPTICAL-FIELD IONIZATION

The mechanism of pump energy absorption and plasma formation is different for gaseous xenon and clustered xenon targets. For a gaseous target the theory [1] predicts that electrons produced by tunneling ionization with circularly polarized light will retain a kinetic energy equal to the quiver energy, $\varepsilon = e^2E^2/4m\omega^2$, after the pulse has finished, where E is the instantaneous electric-field strength at the time of ionization. This is necessary to satisfy conservation of angular momentum at the moment of ionization, which is equivalent. This energy varies from 9 for the first electron ionized to ~550 eV for the eighth electron ionized [2,3]. In this case, the ion velocity is low after laser pulse action.

When considering the interaction of the femtosecond laser pulse with a cluster, the effect of the pulse pedestal interaction with the cluster should be thoroughly explored. This interaction results in rapid heating by inverse bremsstrahlung, followed by rapid expansion of the clusters. The final plasma temperature depends on the cluster size, pedestal pulse duration, and the intensities of the pedestal and main femtosecond pulses. Early experiments [9–12] studied the interaction of intense femtosecond laser radiation with the large (50–200 Å, 10^2–10^7 atoms per cluster) clusters produced in cluster jets. Both experiments and simulations have proved that plasma produced during this interaction exhibits electron temperatures far in excess of that obtained by above-threshold ionization of a low-density gas, i.e., by OFI. Multi-keV electrons were generated in the interaction of intense laser pulses with Xe clusters [12]. Measured mean ion energy reached 10–20 keV

TABLE I. Comparison of atomic data and the gain in the Pd-like xenon, calculated in this work and in Ref. [2].

	This work	Lemoff *et al.* [2]
Radiative decay probability of transition: $4d^9 5p\ ^1P_1 - 4d^{10}\ ^1S_0$ (s^{-1})	$11 \cdot 10^{10}$	$9.3 \cdot 10^{10}$
Radiative decay probability of transition: $4d^9 5d\ ^1S_0 - 4d^9 5p\ ^1P_1$ (s^{-1})	1.3×10^{10}	0.98×10^{10}
Electron energy distribution	Two-hump Maxwell: 91% – $T_e = 70$ eV 9% – $T_e = 500$eV	Non-Maxwell 91% of electrons: from 10 to 100 eV, 9% of 500 eV
Electron-induced transitions: Rates per unit density (cm^3/s):		
$4d^{10}\ ^1S_0 - 4d^9 5p\ ^1P_1$	0.1×10^{-8}	1.3×10^{-8}
$4d^{10}\ ^1S_0 - 4d^9 5d\ ^1S_0$	0.4×10^{-8}	1.5×10^{-8}
$4d^9 5d\ ^1S_0 - 4d^9 5p\ ^1P_1$	1.9×10^{-7}	1.7×10^{-7}
$4d^9 5d\ ^1S_0 - 4d^9 4f\ ^1P_1$	1.5×10^{-7}	3.2×10^{-7}
$4d^9 5d\ ^1S_0 - 4d^9 5f\ ^1P_1$	1.9×10^{-7}	1.7×10^{-7}
Electron collision linewidth ($\lambda = 41.8$ nm) at $n_i = 10^{17}$ cm^{-3}, $n_e = 8 \times 10^{17}$ cm^{-3} (s^{-1})	0.9×10^{11}	1.36×10^{11}
Doppler width (s^{-1})	1.0×10^{11}	0.56×10^{11}
Inversion calculations	Kinetic equations calculations for 55 levels of Xe^{8+}	$N^* = N_i^2(R_{up}\text{-}1/3R_l)(1/\tau_{up} + N_i R_{out})$
Gain (cm^{-1})	16–6 on the interval 1–25 ps	107

[11]. Note that even at such high ion energies, the level widths in Xe^{8+} are determined by the electron-impact broadening. That is caused by large cross sections of transitions induced by electron-ion impacts.

A. X-ray lasers pumped by OFI in gaseous xenon targets

The time evolution of $g(t)$ under experimental conditions [3] is calculated, assuming that after the interaction of the pumping pulse with xenon gas, plasma is formed with the following parameters: $[Xe^{8+}] = 0.9$, $n_e = 3.4 \times 10^{18}$ cm^{-3} (which corresponds to a pressure of 12 torr), and $n_e = n_i \times 8$. In Fig. 2(a) the time evolution of g(t) is shown for two sets of parameters T_e,d : (75 eV,20 μm) and (100 eV,30 μm), respectively. On the right axis of this figure the corresponding emissive powers $I_0(t)$ at 41.8 nm are plotted. From Fig. 2(a), one can see that functions $g(t)$ and $I_0(t)$ reach a maximum in ~1 ps, i.e., this is the time for the upper active level population to a maximum from the ground state by electron impact. The functions $g(t)$ and $I_0(t)$ decay in ~20 ps; decay is caused by the collisional mixing of level populations as well as over Xe^{8+} ionization into Xe^{9+} by electron impact. Figure 2(a) shows the strong dependence of $g(t)$ on T_e (the dependence on d is negligible). The output energy per pulse for plasma cylinder L is calculated by the formula $E_{out} = \tilde{I}_0{}^S \exp(\tilde{g}L)\ t_{las}$, where $\tilde{I}_0{}^S$ is the radiation fraction without regard to lasing directed at the outlet section of the plasma and t_{las} is the lasing duration at 41.8 nm. $\tilde{I}_0{}^S$ is averaged over the time interval t_{las}. The photon yield is $N_{out}^{ph} = E_{out}/E_{ph}$, and the photon energy is $E_{ph} = 29.2$ eV. Dependences of N_{out}^{ph} on L for both calculations are shown in Fig. 2(b), which demonstrates the drastic increase in the yield as T_e increases by only ~ 30%. This effect is unambiguously explained by the large cross section of excitation of the upper active level $4d^9 5d\ ^1S_0$ by electron impact, as well as its strong dependence on T_e.

The XRL in Ref. [4] generates 5×10^9 photons per pulse with a saturation length of ~5 mm. These data were sufficient to reproduce the experimental results with our theoretical model. Close agreement is reached with $T_e = 140$ eV, $n_e = 4.8 \times 10^{18}$ cm^{-3}, and effective diameter $d = 16$ μm. We believe that at higher intensities [4] at the initial instant, xenon is in a higher ionization stage than in Ref. [3]; this is accounted by the value $[Xe^{8+}] = 0.85$. The calculated $g(t)$ and $I_0(t)$ are shown in Fig. 3(a). The corresponding length dependence of the calculated 41.8 line emission is shown in Fig. 3(b).

B. X-ray lasers pumped by OFI in xenon cluster jets

In the experiment [5] with the slit nozzle for cluster jet formation, strong x-ray lasing was achieved without prepulse, and the average atomic density was measured to be in the range of 1.1×10^{17} to 3.3×10^{19} cm^{-3}. The optimal atom density was found for a fixed $L = 1.7$ mm. The lasing plasma diameter was assumed to be $d = 25\mu$m. The lasing intensity as a function of the average atomic density is shown in Fig. 3 of Ref. [5]. The lasing signal maximum appears at

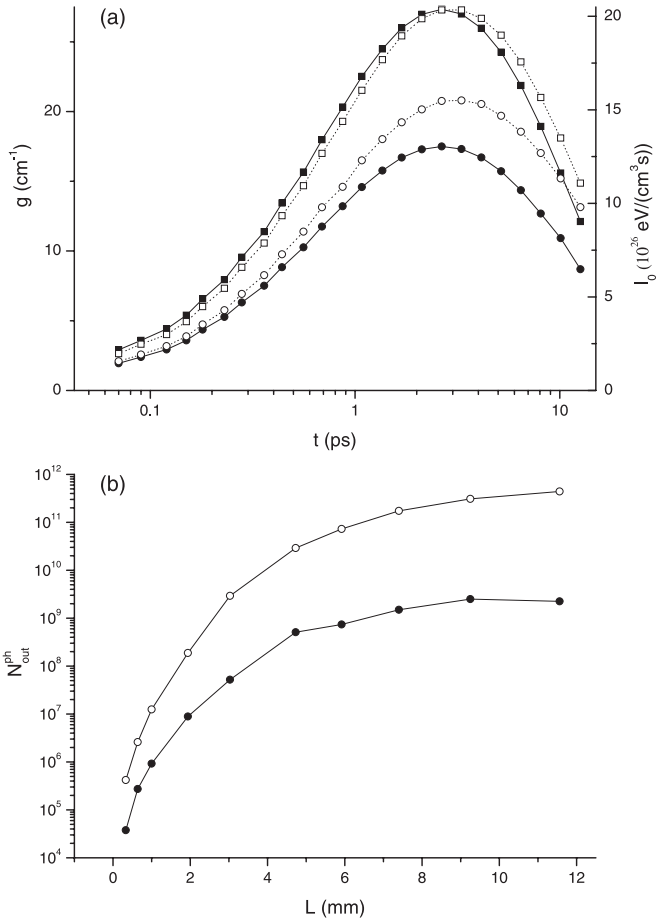

FIG. 2. (a) Time evolution of the gain $g(t)$ for the transition $4d^9{}_{5/2}5d_{5/2}\ {}^1S_0{-}4d^9{}_{5/2}5p_{3/2}\ {}^1P_1(\lambda = 41.8$ nm) in Xe^{8+} in plasma with $n_e = 3.4 \times 10^{18}$ cm^{-3} (solid curves): $T_e = 75$ eV,d = 20 μm(•) : $T_e = 100$eV,d = 30 μm(■). The corresponding time evolution of the power emissivity per unit volume $I_0(t)$ is shown on the right axis by dashed curves: $T_e = 75$ eV,d = 20 μm(○),$T_e = 100$eV,d = 30 μm(□). (b) Length dependence of the calculated 41.8-line emission at $n_e = 3.4 \times 10^{18}$ cm^{-3}: $T_e = 75$ eV,d = 20 μm(•),$T_e = 100$ eV, $d = 30$ μm(○).

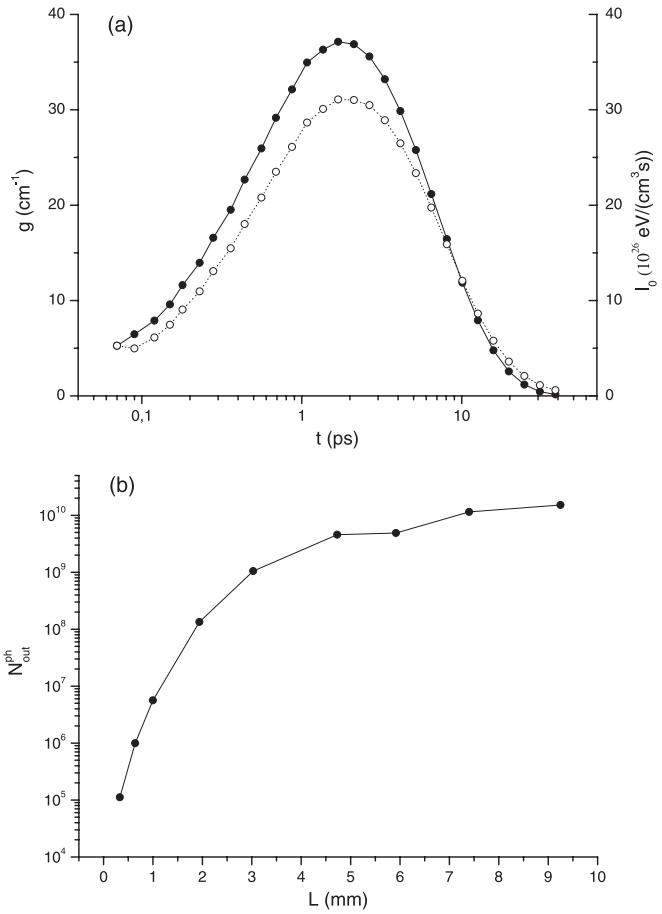

FIG. 3. (a) Time evolution of the gain $g(t)$ at $\lambda = 41.8$ nm in a plasma with parameters fitted for the experiment [4]: $n_e = 4.8 \times 10^{18}$ cm^{-3}, $T_e = 140$ eV, $d = 16$ μ m, and $[Xe^{8+}] = 0.85$ (•). The corresponding time evolution of the power emissivity per unit volume $I_0(t)$ is shown on the right axis (○). (b) Length dependence of the calculated 41.8-line emission at plasma parameters of Fig. 3(a).

an atomic density of 7.5×10^{17} cm^{-3}, and the lasing line reached 2×10^{10} photons per pulse (95 nJ). In interpreting these results, we calculated the quantum yields for each atomic density as shown in Fig. 3 of Ref. [5]. Calculations were performed with the following fixed parameters: $d = 25\mu m$, $L = 1.7$ mm, $[Xe^{8+}] = 0.9$, and $n_e = 8n_i$. For each atomic density T_e was chosen so as to reproduce the function of the lasing signal dependence on the atomic density as shown in Fig. 3 of Ref. [5]. The results of our calculations for the photon yield at 41.8 nm are shown in Fig. 4. The dependence of T_e on the atomic density determined in such a way is given on the right axis of Fig. 4. T_e increases from 310 to 1100 eV as the atom density increases from 10^{17} to 6×10^{18} cm^{-3} ($7.2 \times 10^{17} \leqslant n_e \leqslant 4 \times 10^{19}$ cm^{-3}). The T_e increase with increasing atomic density is consistent with the results shown in the inset of Fig. 3 in Ref. [5]. Based on the above calculations we can assert that a noticeable laser effect can be achieved if $T_e \geqslant 2$ keV at $n_e \sim 4 \times 10^{20}$ cm^{-3} ($n_i = 3 \times 10^{19}$ cm^{-3}).

IV. THE OPTIMIZATION OF X-RAY LASERS PUMPED BY OFI IN XENON CLUSTER JETS

XRL pumped by OFI of gaseous xenon targets are necessary to test our model. Their study stopped due to little absorption of E_{pump} in a gas medium, which is less than 0.1%. Early experiments [9–12] studied the interaction of intense femtosecond laser radiation with the large (50–200 Å, 10^2–10^6 atoms per cluster) clusters produced in cluster jets. The energy absorption efficiency by noble-gas clusters was measured in Ref. [9]. It was found that with a peak laser intensity of 7×10^{16} W/cm^2, the energy absorption efficiency could reach as high as 95% for xenon clusters. Multi-keV electrons were generated in the interaction of intense laser pulses with Xe clusters [12]. The interpretation of the XRL pumped by OFI in a cluster jet along with an analysis of the way to obtain the maximum possible yield is aimed to justify the principles of highly efficient tabletop XRL at 41.8 nm.

Independent experiments [13,14] have discovered the way to a new generation of x-ray lasers. These experiments on the interaction between the optical field of a high-intensity laser pulse with a xenon cluster jet revealed an anomalously high quantum yield in the range of 10–15 nm in Xe^{26+}. For

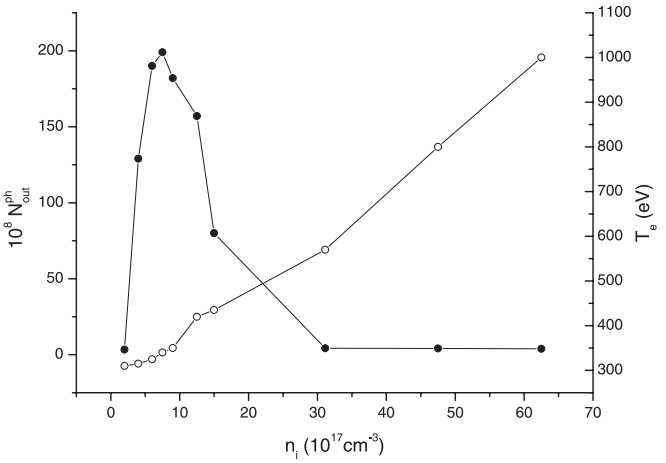

FIG. 4. Photon yield (•) at 41.8 nm as a function of the atomic density n_i in plasma with $L = 1.7$ mm, $d = 25$ μm. T_e (○, right axis) was determined by fitting the calculated quantum yields to the corresponding experimental yields shown in Fig. 3 of Ref. [5].

$\lambda = 13.4 \pm 2.2$ nm the pump energy conversion coefficient into this line intensity was about 0.5% in 2π sr in both experiments. In Ref. [8] we have developed a model of high-intensity monochromatic radiation source with $\lambda = 4$, 10, 11.3, and 13–13.9 nm on transitions in Ni-like xenon. The plasma was assumed to be formed as a result of the interaction of a xenon cluster jet with an ultrashort laser pulse. Within this model we determined the plasma filament density, temperature, diameter, and length; these parameters turned out to be in good agreement with the corresponding experimental data. The energy yield at the wavelength in the range of 10–15 nm, calculated in Ref. [8], was also in good agreement with the experimental results.

A. Optimization of electron density in plasma for XRL in Xe^{8+}

We start the consideration with fixing $L = 1.5$–2 mm, since this length is most suitable for an experimental work as well as in terms of minimizing the spatial divergence of the XRL. From this value of L it follows that the XRL duration τ_{las}, i.e., the decay time of $g(t)$ should be ~5–6 ps. It follows from our calculations that this condition is satisfied at $n_e \approx 10^{19}$ cm^{-3} (the decay time is approximately inversely proportional to n_e). The time evolution of $g(t)$ at $n_e = 10^{19}$ cm^{-3}, $d = 25\mu$ m, and $[Xe^{8+}] = 0.9$ is shown in Fig. 5(a) for three values of T_e: 420, 550, and 900 eV. The corresponding $g(t)$ averaged over 5.1 s (1.7 mm) are $\tilde{g} = 61.9$, 78.5, and 116.7 cm^{-1}, respectively. The photon yield as a function of T_e is given in Fig. 5(b). $T_e =$ 430 eV was defined in our calculation (Fig. 4) as T_e obtained in Ref. [5] for $n_e = 10^{19}$ cm^{-3} ($n_i \approx 1.1 \times 10^{18}$ cm^{-3}).

B. Optimization of electron temperature in plasma for XRL in Xe^{8+}

In experiment [4], a twofold increase in I_{pump} resulted in an increase in N_{out}^{ph} by about three orders of magnitude, which confirms our conclusion about the extremely strong dependence of N_{out}^{ph} on T_e.

Thus, T_e is a key parameter to achieve maximum yield of XRL in Xe^{8+}. The experimental measurements of scaling

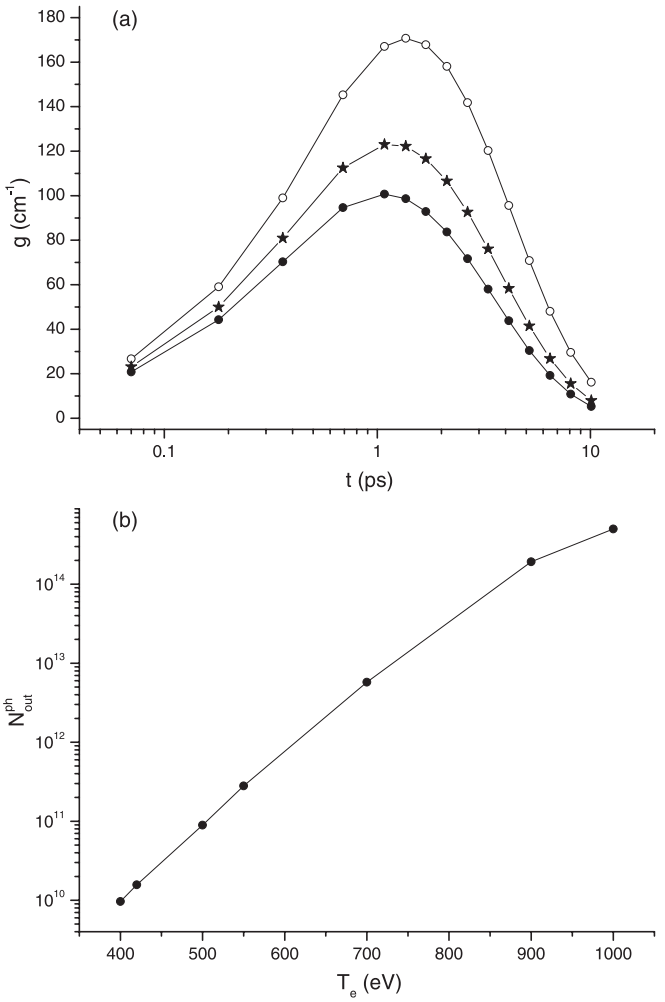

FIG. 5. (a) Time evolution of the gain at $\lambda = 41.8$ nm in plasma with $n_e = 10^{19}$ cm^{-3} ($n_i \approx 1.1 \times 10^{18}$cm^{-3}),d = 25$\mu$m,$T_e$ = 420eV(•),T_e = 550 eV (⋆), and T_e = 900eV(○). (b) Dependence of the quantum yield of the x-ray laser on the electron temperature at $n_e = 10^{19}$ cm^{-3},$d = 25\mu$m.

with cluster sizes and laser parameters of the energies of ions and electrons produced in the explosion of clusters were obtained in Ref. [11]. Ion (and electron) energies scaling with cluster size (ranging from 10^2 to 10^5 atoms per cluster), laser intensity 10^{14} –10^{16} W/cm^2, and laser wavelengths 780 and 390 nm were presented for Xe and Kr clusters. Figure 3 of Ref. [11] shows the increase of ion energies with cluster size. The electron energy was in the range 0.3–2 keV in Ref. [11]. In experiment [12], a Ti:sapphire laser system was used delivering 40 mJ, 150 fs pulses at a wavelength 780 nm with a peak intensity ~10^{16} W/cm^2. The xenon jet was operated with a backing pressure range from 0 to 5 bars. The low pressure along with nozzle parameters provided quite small xenon cluster size 1000–2000 atoms per cluster (50 Å). The kinetic-energy distribution in Ref. [12] consisted of two features: a "warm" peak of between 0.1 and 1 keV and a "hot" peak of energy between 2 and 3 keV.

Apparently, T_e increase with increasing atomic density is due to an increase in cluster size with increasing backing pressure. The clusters in the jet produced by the slit nozzle

in Ref. [5] proved to be larger than those produced by the conical nozzle. Thus, T_e in plasma, produced using the slit nozzle is higher than that using the conical nozzle, when all the parameters for Xe gas in the backing camera are the same for both types of nozzles.

The nanoplasma model suggests [11] that the point in the laser pulse at which the cluster experiences resonant heating governs the dynamics of the cluster explosion. The highest electron temperature is obtained when the cluster nanoplasma density passes through the $3n_{\rm crit}$ point close to the laser pulse peak; $n_{\rm crit} = \pi c^2 m_e/e^2\lambda^2$ is the electron density at which the laser frequency is equal to the plasma frequency. Cluster nanoplasma density increases under the interaction with a pedestal part of the main femtosecond pulse. Note that small clusters expand more rapidly and reach this point before the peak; too large clusters pass through $3n_{\rm crit}$ well after the peak. The sharp "hot electron" peak in the electron energy distribution is due to electrons which leave the cluster at the $3n_{\rm crit}$ resonance.

C. Justification of the use of a conical mirror (axicon) as a plasma waveguide

A serious problem for longitudinally pumped gas-cluster–target XRL is the limited gain length caused by ionization-induced refraction. In our previous work [7] we discussed the critical role of axicon for the formation of uniform plasma with a given length L.

Among all of the guiding methods reported, optically preformed plasma waveguide in a cluster jet is most favorable [15–17] because it allows (1) reduced ionization-induced refraction due to transformation of the Gaussian profile of a pump pulse to Bessel one; (2) guiding of the pump pulse and the lasing x-ray pulse simultaneously; (3) characterization of the underlying process through various diagnostics such as interferometry; and (4) damage-free long-term high-repetition-rate operation for practical applications. In experiment [18], a krypton plasma waveguide was prepared by using the axicon-ignitor-heater scheme. in Ref. [18] the XRL at 32.8 nm on the transition $3d^9 4d\ ^1S_0$–$4d^9 4p\ ^1P_1$ in Ni-like krypton was studied. A dramatic enhancement of XRL was achieved: 400 folds relative to the case without a plasma waveguide.

D. Range of variation of plasma parameters

Optimization of the XRL described above is performed for plasma parameters of the experiment [5]. This approach requires a very modest power pump laser. However, in this experiment plasma filament was chosen, as thin as 25 μ m. That is fraught with considerable destruction of plasma due to interaction with outside clusters, and consequently, considerable radial nonuniformity of plasma. This problem was discussed in Ref. [5] (see inset of Fig. 3 in Ref. [5]). Obviously, the uniformity of plasma will be improved if d is increased to ~100–200 μm.

XRL with a highest possible conversion can be created in a wide range of density: $10^{17} \leqslant n_e \leqslant 1.25 \times 10^{19}{\rm cm}^{-3}$ with lasing duration in limits $10^3 \geqslant \tau_{\rm las} \geqslant 3$ ps, which correspond to the optimum plasma length in limits $30 \leqslant L \leqslant 0.1$ cm. At low density ($n_e < 10^{17}$ cm^{-3}) the mixing of level populations by electron impact is negligible (this is coronal approximation); even at very low $T_e \sim 30$ eV the inversion of active levels is positive. Our preliminary calculations have shown that at $n_e \approx 10^{17}$ cm^{-3}, $T_e \approx 50$–75 eV, $\tau_{\rm las} \approx 1$ ns, and $L \approx 20$–30 cm the averaged $\tilde{g} \approx 1$ cm^{-1} [19]. At this plasma density $g(t)$ reaches the maximum value at 50–100 ps. In this case d can be large enough, so that the erosion of the outer layer of plasma may be relatively small. Thus, the change of refractive index at the edge of the plasma does not lead to a strong divergence of the amplified extreme ultraviolet (EUV) beam, as was the case in the experiments [5] where $d \approx 25$ μm. The formation of low-density plasma in a volume of ~5 cm^3 requires ~ 4–5 J with the possible use of the pump laser at the duration of several picoseconds and an intensity $\geqslant 10^{14}$W/cm^2.

The influence of laser pulse width on absolute EUV yield from Xe clusters was studied in Ref. [20]. Absolute yield measurements of EUV emission in Xe^{26+} in a wavelength range between 10 and 15 nm in combination with a cluster-target variation were carried out. Our calculations [8] have shown that a time duration of EUV emission in the range

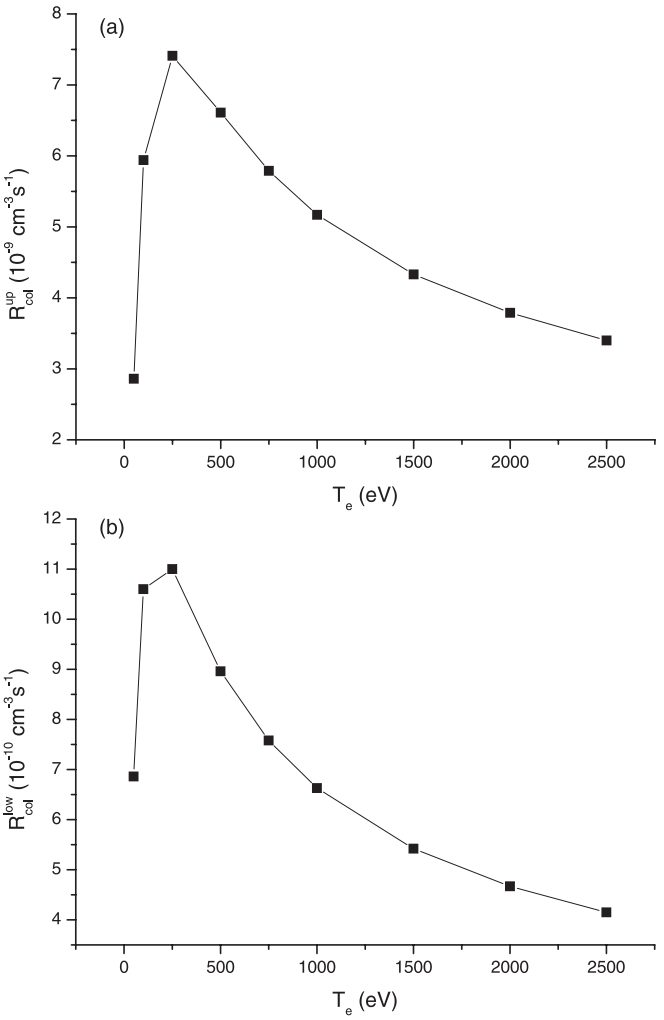

FIG. 6. Rate coefficients ($R_{\rm col}$) of electron-impact excitations per unit volume as functions of T_e for the upper $4d^9 5d\ ^1S_0$ (a) and the low $4d^9 5p\ ^1P_1$ (b) active levels.

10–15 nm under the experimental conditions of Ref. [14], [20] was $\leqslant$5 ps. In experiment [20] 50 fs ($I_{\text{pump}} \sim 2 \times 10^{18}$ W/cm^2) and 2 ps ($\sim 5 \times 10^{16}$W/cm^2) pulses from a Ti:sapphire multi-TW laser at 800 nm were used for plasma formation by an interaction with large Xe clusters (10^5–10^6 atoms per cluster). The picosecond-laser pulse resulted in an ~30% enhanced and spatially more uniform EUV emission compared to femtosecond-laser excitation. Using a 2 ps pulse the absolute emission efficiency at 13.4 nm of up to 0.8% in 2π sr and 2.2% bandwidth has been obtained.

With increasing plasma density, a higher T_e value is required for maximum yield (see Fig. 4). The maximum possible yield of the XRL in Xe^{8+} (conversion ~0.5% from the pump pulse energy) is possible for $n_e \approx 10^{19}$, $T_e \approx 1000$ eV. A further increase of density leads to a decrease of conversion for any (arbitrarily high) T_e. The reason can be understood from the functions of the rate of excitation of active levels by electron impact shown in Figs. 6(a) and 6(b). Functions $R_{\text{col}}(T_e)$ have a maximum at 300–500 eV and decrease at $T_e \geqslant 500$ eV. XRL with a lower conversion is possible at $1.25 \times 10^{19} \leqslant n_e \leqslant (2.5) \times 10^{20}$cm^{-3}([Xe] $\leqslant 3.2 \times 10^{19}$ cm^{-3}).

V. CONCLUSION

In recent years research was conducted of XRL pumped by OFI in cluster jets of krypton. Laser effect and quantum yield were studied on the 4*d*-4*p* transition in Kr^{8+} with $\lambda = 32.8$ nm [18,21]. In the present paper the choice of XRL in Xe^{8+} is conditioned by the presence of experimental results obtained in the two different approaches [3–5]. The approach in Ref. [5] is promising to construct high-efficiency XRL, provided that plasma parameters (L,d,t_{las},n_e,T_e) will be optimized (i.e., they should be consistent with each other). Also, a way should be found to reach a sufficiently high value of T_e.

Our model can adequately reproduce the experimental values of $N_{\text{out}}^{\text{ph}}$ by adjusting the plasma parameters T_e,d, and [Xe^{8+}]. We have found that in experiments using OFI of gas xenon targets, the diameter of plasma with appropriate parameters for lasing is smaller than the Airy-Gauss intensity distribution in the focal plane. The strong dependence of $N_{\text{out}}^{\text{ph}}$ on T_e is due to the large cross section and rate coefficient of excitations of the upper active level $4d^9 5d\ ^1S_0$ by electron impact [see Table I and Fig. 6(a)]. The inversion increases rapidly with T_e if $T_e \leqslant 1000$ eV. It seems urgent to experimentally study the cross sections of level excitations and radiative transition probabilities in Xe^{8+}.

As can be seen in Figs. 2(a), 3(a), and 5(a), the upper active level is populated in ~1 ps. Thus, we can assert that at this density, the hot electron production due to scattering on hot ions may be of the order of ~1 ps. We believe that appreciably larger T_e (and $N_{\text{out}}^{\text{ph}}$) in comparison with experiment [5] could be achieved if the necessary conditions are satisfied: (i) production of larger-size clusters in a jet, which can be achieved by decreasing the xenon temperature in the backing camera as well as the opening angle producing the jet profile, etc.; (ii) optimization of the duration and intensity of the pump pulse pedestal to provide the resonance interaction of nanoplasma in the cluster with peak of pulse; (iii) use of a conical mirror (axicon) as a plasma waveguide, i.e., using a waveguide, maintaining a sufficient pump intensity over a necessary distance, the size of the underionized absorptive region can be reduced; (iv) the main pulse intensity should be ~10^{16} W/cm^2 as sufficient to eight-time ionize atom xenon [3,4]; $E_{\text{pump}} \geqslant 1$ mJ, its value is dependent on plasma size; and (v) use of a circularly polarized laser pump pulse, which is efficient as applied to the OFI of the atomic shells 5*s*, 5*p*.

The highly efficient XRL pumped by OFI in a xenon cluster jet with a yield ~0.5% at 41.8 nm is feasible using an appropriate nozzle in a wide range of plasma parameters using femtosecond or picosecond lasers.

In our work [8] we suggested using a slit nozzle for XRL pumped by OFI in a cluster jet. The experimental results of Ref. [5] showed an advantage of the slit nozzle for the plasma formation, i.e., with a slit nozzle more suitable conditions for laser effect were obtained. We believe that with equal pressure and temperature of gas in a back camera as well as an equal opening angle in a nozzle, the cluster size is larger in the case of a slit nozzle. This results in larger T_e in plasma and larger $g(t)$ values. Unfortunately, so far there is no analog of the Hagena formula in the annex to the slit nozzles. We believe it is urgent to search for the phenomenological formula for estimating the cluster size in a cluster jet as a function of gas pressure and temperature in a back camera, as well as of an opening angle in a slit nozzle.

[1] P. B. Corkum, N. H. Burnett, and F. Brunel, Phys.Rev. Lett. **62**, 1259 (1989).

[2] B. E. Lemoff, C. P. J. Barty, and S. E. Harris, Opt. Lett. **19**, 569 (1994).

[3] B. E. Lemoff, G. Y. Yin, C. L. Gordon, C. P. J. Barty, and S. E. Harris, Phys. Rev. Lett. **74**, 1574 (1995).

[4] S. Sebban *et al.*, Phys. Rev. Lett. **86**, 3004 (2001).

[5] H.-H. Chu, H.-E. Tsai, M.-C. Chou, L.-S. Yang, J.-Y. Lin, C.-H. Lee, J. Wang, and S.-Y. Chen, Phys. Rev. A **71**, 061804(R) (2005).

[6] K. G. Whitney, A. Dasgupta, and P. E. Pulsifer, Phys. Rev. E **50**, 468 (1994).

[7] E. P. Ivanova, Phys. Rev. A **82**, 043824 (2010).

[8] E. P. Ivanova and A. L. Ivanov, J. Exp. Theor. Phys. **100**, 844 (2005).

[9] T. Ditmire, R. A. Smith, J. W. G. Tisch, and M. H. R. Hutchinson, Phys. Rev. Lett. **78**, 3121 (1997).

[10] T. Ditmire, T. Donnelly, A. M. Rubenchik, R. W. Falcone, and M. D. Perry, Phys. Rev. A **53**, 3379 (1996).

[11] E. Springate, N. Hay, J. W. G. Tisch, M. B. Mason, T. Ditmire, M. H. R. Hutchinson, and J. P. Marangos, Phys. Rev. A **61**, 063201 (2000).

[12] Y. L. Shao, T. Ditmire, J. W. G. Tisch, E. Springate, J. P. Marangos, and M. H. R. Hutchinson, Phys. Rev. Lett. **77**, 3343 (1996).

[13] M. Mori, T. Shiraishi, E. Takahashi, H. Suzuki, L. B. Sharma, E. Miura, and K. Kondo, J. Appl. Phys. **90**, 3595 (2001).
[14] S. Ter-Avetisyan, U. Vogt, H. Stiel, M. Schnürer, I. Will, and P. V. Nickles, J. Appl. Phys. **94**, 5489 (2003).
[15] C. G. Durfee, J. Lynch, and H. M. Milchberg, Phys. Rev. E **51**, 2368 (1995).
[16] P. Volfbeyn, E. Esarey, and W. P. Leemans, Phys. Plasmas **6**, 2269 (1999).
[17] Y.-F. Xiao *et al*., Phys. Plasmas **11**, L21 (2004).
[18] M. C. Chou, P.-H. Lin, C.-A. Lin, J.-Y. Lin, J. Wang, and S.-Y. Chen, Phys. Rev. Lett. **99**, 063904 (2007).
[19] E. P. Ivanova, in *X-Ray Laser 2002: 8th International Conference on X-Ray Lasers*, edited by J. J. Rocca *et al*. (AIP, Melville, NY, 2002).
[20] M. Schnürer, S. Ter-Avetisyan, H. Stiel, U. Vogt, W. Radloff, M. Kalashnikov, W. Sandner, and P. V. Nickles, Eur. Phys. J. D **14**, 331 (2001).
[21] P.-H. Lin, M.-C. Chou, C.-A. Lin, H.-H. Chu, J.-Y. Lin, J. Wang, and S.-Y. Chen, Phys. Rev. A **76**, 053817 (2007).